Identification of *sur2* mutation affecting the lifespan of fission yeast

Tatsuhiro Kurauchi[1]*, Kotaro Matsui[1]*, Takafumi Shimasaki[1], Hokuto Ohtsuka[1], Satoshi Tsubouchi[2], Kunio Ihara[3], Motohiro Tani[4], and Hirofumi Aiba[1¶]

1. Laboratory of Molecular Microbiology, Department of Basic Medicinal Sciences, Graduate School of Pharmaceutical Sciences, Nagoya University, Chikusa-ku, Nagoya 464-8601,Japan
2. Laboratory of Molecular Microbiology, Graduate School of Bioagricultural Sciences, Nagoya University, Chikusa-ku, Nagoya 464-8601, Japan
3. Center for Gene Research, Nagoya University, Chikusa-ku, Nagoya 464-8601, Japan
4. Department of Chemistry, Faculty of Sciences, Kyushu University, Nishi-ku, Fukuoka 819-0395, Japan

* These authors have contributed equally to this work.

¶Corresponding author; Hirofumi Aiba, Laboratory of Molecular Microbiology, Department of Basic Medicinal Sciences, Graduate School of Pharmaceutical Sciences, Nagoya University, Chikusa-ku, Nagoya 464-8601, Japan. Tel. 81-52-747-6803, Fax: 81-52-747-6806, E-mail: aiba@ps.nagoya-u.ac.jp

Running head: chronological lifespan of fission yeast

Abstract

Yeast is a suitable model system to analyze the mechanism of lifespan. In this study, to identify novel factors involved in chronological lifespan, we isolated a mutant with a long chronologically lifespan and found a missense mutation in the *sur2*$^{+}$ gene, which encodes a homolog of *S. cerevisiae* sphingolipid C4-hydroxylase in fission yeast. Characterization of the mutant revealed that loss of *sur2* function resulted in an extended chronological life span. The effect of caloric restriction, a well-known signal for extending lifespan, is thought to be dependent on the *sur2*$^{+}$ gene.

Key words

Lifespan, *Schizosaccharomyces pombe*, Aging, Sphingolipid hydroxylase, Sur2, Yeast

Introduction

In yeast, the chronological lifespan is defined as the period during which the cell maintains viability after entering stationary phase (Roux *et al*., 2010). In *Saccharomyces cerevisiae*, the PKA pathway and the Sch9 pathway have been identified that control chronological lifespan (Fabrizio and Longo, 2003; Fabrizio *et al*., 2001). Down-regulation of either pathway promotes lifespan extension. In higher eukaryotes, a similar pathway (insulin/IGF-I-like) regulates lifespan, suggesting a common evolutionary origin for lifespan regulation (Longo and Fabrizio, 2002; Longo and Kennedy, 2006). In *Schizosaccharomyces pombe*, Pka1 and Sck2 are regulators of chronological lifespan, with mutants of each showing a long-lived phenotype, and double mutant of *pka1* and *sck2* having an additive effect on chronological lifespan, suggesting that these two factors regulate related but independent pathways (Roux *et al*., 2006). Information on factors involved in the regulation of lifespan in fission yeast has been accumulated (Ohtsuka *et al*., 2020).

In order to understand the mechanisms controlling chronological lifespan, we have identified and analyzed several mutants that exhibit long or short-lived phenotype in fission yeast. These variants can be broadly classified into those involved in glucose utilization (Ito *et al*., 2010; Naito *et al*., 2014; Kurauchi *et al*., 2017) and those involved in cell surface structure (Oshiro *et al*., 2003; Fujita *et al*., 2007; Imai *et al*., 2020).

Since lifespan is thought to be intricately regulated by many factors, and factors important for lifespan regulation are conserved in eukaryote, understanding lifespan regulation requires the identification of new factors that affect lifespan at different stages. We therefore searched for and characterized lifespan extending mutant of *S. pombe*.

Materials and Methods

Strain and media- S. pombe strain JY333 (*h⁻ leu1-32 ade6-M216*) was used for mutant screening. *S. pombe* strain HM3802 (*h⁺ leu1-32 ade6-M210*) was used for backcrossing, and the JY333 *sur2-L1::kan^{R}* strain was generated using the *kan*^{r} cassette derived from pFA6a-kanMX6 (Bähler *et al.*, 1998). The following oligonucleotides were used to transform the L1 mutant by electroporation with DNA fragments amplified by PCR: F1:CTTCATCATTGACAGCTGGC; F2:TTAATTAACCCGGGGATCCGTAAAACGCGTCTACGATACC; R1:CTGACTTATGCGACCTCGAC; R2:GTTTAAACGAGCTCGAATTCTAACTTACTGTAAACACGGG. The GST cassette from pFA6a-GST-kanMX6 was used to produce the Sur2-GST and Sur2-L1-GST strains (Bähler *et al.*, 1998). Oligonucleotides were used and DNA fragments amplified by PCR were used to transform JY333 and L1 mutant by electroporation. F1:CTTCATCATTGACAGCTGGC; F2:TTAATTAACCCGGGGATCCGGTTAACCTTCTTTGCATTCTTAGCC; R1:CTGACTTATGCGACCTCGAC; R2:GTTTAAACGAGCTCGAATTCGGTAGTACAAATCGATTGGC. SD medium (0.67 % yeast nitrogen base without amino acids [Difco], 2 % glucose) or YE medium (0.5 % yeast extract [Difco], 3 % glucose) with standard amounts of the components necessary for growth were used for the cultivation at 30 ˚C. Analysis of viability was performed as described previously (Ohtsuka *et al.*, 2008, Kurauchi *et al.*, 2017). For caloric restriction experiment, SD low glucose medium (SD medium containing 0.5% glucose) was used. For caffeine or KCl sensitivity tests, logarithmic growth phase cells were spotted in serial dilutions onto YE plates containing 1M KCl or 10 mM caffeine and the plates were incubated at 30 °C for 3 days.

Western blot analysis- Strains Sur2-GST (*h⁻ leu1-32 ade6-M216 sur2-GST::kan*^{R}) and Sur2-L1-GST (*h⁻ leu1-32 ade6-M216 sur2-L1-GST::kan*^{R}) were grown in SD medium. At the logarithmic growth phase, cells were

collected and cell lysates were prepared. After SDS polyacrylamide gel electrophoresis, the amounts of Sur2 or Sur2-L1 protein was detected with anti GST antibody (Santa Cruz Biotechnology). Tubulin was detected as loading control.

Plasmid construction- To overexpress wild type Sur2, pSur2 plasmid was constructed. Two oligonucleotides were used to amplify the *sur2*$^{+}$ gene region. The amplified DNA fragment was digested with the restriction enzymes *Pst*I and *Sal*I, and then cloned into the vector plasmid pLB-Dblet to construct pSur2.
Forward:TAGCTGCAGCAAGTGTCCTTCGTAGTCGC;
Reverse:TCAGTCGACGTCACGTCTGTCACCACCAG.

Library construction and whole genome resequencing- Genome sequencing of L1 mutant was performed essentially as described (Kurauchi *et al.*, 2017).

Extraction of lipids and TLC analysis- Extraction of lipids and TLC analysis were basically carried out as described by Nakase *et al*., 2010. Cells cultured in SD medium were diluted in fresh SD medium (1.0 OD_{600} units/ml (*S. pombe*) or 0.3 OD_{600} units/ml (*S. cerevisiae*)) and incubated at 30°C for 5 hours. Cells (3.5 OD_{600} units) were collected, washed with water, suspended in 350 µl of ethanol/water/diethyl ether/pyridine/15 M ammonia (15 : 15 : 5 : 1 : 0.018, by vol.) and incubated at 65 °C for 15 min. The lipid extract was centrifuged at 10,000 g for 1 min and extracted once more in the same way. The supernatant liquid obtained was dried and treated with weak alkali using monomethylamine (MMA). For this purpose, the lipid extract was dissolved in 130 µl MMA [40 % methanol solution/water (10 : 3, by vol.)], incubated at 53 °C for 1 h and then dried. The lipids were suspended in 50 µl of chloroform/methanol/water (5 : 4 : 1, by vol.), incubated at 60 °C for 2 min and then separated on silica gel 60 TLC plates (Merck) using chloroform/methanol/4.2 M ammonia (9 : 7 : 2, by vol.) as the solvent system. The TLC plates were sprayed with 10 % copper sulphate dissolved in 8 % orthophosphoric acid and heated at 180 °C to visualize sphingolipids. The identification of each sphingolipid band was performed as described in a previous study (Uemura *et al.*, 2014).

Results and Discussion

Identification of a long-lived mutants that extend their chronological lifespan. We have previously screened long-lived mutants of *S. pombe* (Ito *et al*., 2010), and in this study we analyzed one unidentified mutant, which we named L1. First, we analyzed the long-lived phenotype of L1 (Fig.1A): the L1 mutant maintained viability longer than the wild type even after entering stationary phase; the doubling time of L1 and JY333 in the logarithmic growth phase was almost the same, 3.12 h and 3.16 h, respectively. We found one mutation in the ORF of the *sur2*$^{+}$ gene (SPBC887.15c) that caused a substitution from Ala-196 to Val (Figs. 1B and 2A). We named this mutation the *sur2-L1* mutation. The *sur2*$^{+}$ gene encodes a homologue of *S. cerevisiae* sphingolipid C4-hydroxylase.

We then confirmed that the identified mutation (designated *sur2-L1* allele) is the mutation responsible for the longevity phenotype of the L1 mutant, as follows. First, the L1 mutant was crossed with a wild type strain (HM3802) to obtain progeny. Long-lived cells (n = 4) and non-long-lived cells (n = 6) were randomly selected and sequenced in the chromosomal region corresponding to the *sur2-L1* mutation. The results confirmed that long-lived cells have the *sur2-L1* mutation and non-long-lived cells have the wild type *sur2*$^{+}$ allele. Representative sequencing data for each cell are shown in Fig. 1B. Next, the identified GCT to GTT mutation causing the change from Ala-196 to Val was introduced into the wild type *sur2*$^{+}$ gene on the chromosome. The constructed *sur2-L1*::*kan*^{R} mutant showed the same long-lived phenotype as seen in the original L1 mutant (Fig. 2A and 2B). Finally, a multicopy plasmid carrying the *sur2*$^{+}$ gene was introduced into the L1 mutant and its lifespan was analyzed by spotting. As shown in Fig. 2C, the longevity phenotype of the L1 mutants was somewhat returned to normal by the introduction of the plasmid pSur2 carrying *sur2*$^{+}$ gene. From these results, we conclude that *sur2-L1* is the mutation responsible for the long-lived phenotype of the L1 mutant.

It should be noted that the lifespan was slightly extended when pSur2 was introduced in the wild strain background (Fig.2C). As described later, we conclude that the *sur2-L1* mutation is almost a loss-of-function mutation. These results suggest that a normal amount of Sur2 protein is required to maintain a normal lifespan, and that imbalance due to decreased or increased Sur2 activity may extend lifespan.

Properties of the sur2-1 mutant. Because the *sur2-L1* mutation found here is in the hydroxylase domain

of the Sur2 protein, we predicted that the enzymatic activity of the Sur2-L1 protein would be lost or reduced (Fig.3A). To confirm this, we first fused a GST-tag to the C-termini of the Sur2 and Sur2-L1 proteins on the chromosome, respectively, and analyzed the amount of Sur2-L1 protein expressed from the *sur2-L1* locus by Western blotting with an anti-GST antibody. As shown in Fig.3B, there was no difference in the amount of Sur2 protein and Sur2-L1 protein, indicating that the stability of both proteins is basically the same. Next, the composition of sphingolipids was monitored by TLC analysis to evaluate the enzyme activity (Nakase *et al*., 2010, Kondo *et al*., 2014). In this experiment, wild type and *sur2*Δ mutant of *S. cerevisiae* were used as controls for the composition of sphingolipids. Samples of wild type, *sur2-L1*::*kan*^{R} mutant and *sur2*Δ mutant of *S. pombe* were then analyzed in parallel with the samples of *S. cerevisiae*. As shown in Fig. 3C, the composition of sphingolipids was different between *S. cerevisiae* and *S. pombe*. The main type of sphingolipid was inositol phosphorylceramide (IPC)-C in wild type *S. cerevisiae* and mannosylinositol phosphorylceramide (MIPC)-C in wild type *S. pombe*. The most striking difference in *S. pombe sur2*Δ cells was the accumulation of IPC-C. The structures of sphingolipid and their biosynthesis pathways in *S. cerevisiae* are shown in Fig. S1 (Nakase *et al*., 2010). Orthologous relationships of sphingolipids biosynthetic genes between *S. pombe* and *S. cerevisiae* are summarized in Fig. S2.

On the other hand, the *sur2-L1*::*kan*^{R} mutant and the *sur2*Δ mutant of *S. pombe* had a similar composition of sphingolipids but differed from wild type cells, suggesting that the *sur2-L1* mutation is essentially a loss-of-function mutation. If so, then the *sur2*Δ mutant should also show a long-lived phenotype, and this was confirmed as shown in Fig. 4A. As expected, the *sur2*Δ mutant showed a long-lived phenotype. We also analyzed the different phenotypes between the *sur2*Δ and *sur2-L1*::*kan*^{R} mutant (Fig. 4B). *sur2*Δ mutant was sensitive to KCl (1M) and caffeine (10mM), and these phenotypes were also observed in the *sur2-L1*::*kan*^{R} mutant, but the phenotype was weaker compared to the *sur2*Δ mutant. From these results, we conclude that Sur2 function is severely, but not completely, lost in the *sur2-L1* mutant.

Here we noticed that the phenotype observed in the *sur2*Δ mutant is similar to that of the *pka1*Δ mutant (Fig. S3), and that the *pka1*Δ mutant itself has been reported to be long-lived. To elucidate the genetic interaction between *pka1*$^{+}$ and *sur2*$^{+}$, we generated a *pka1*Δ *sur2*Δ double mutant and analyzed its phenotype. As shown in Fig. 5A, the *pka1*Δ mutant was long-lived, as previously known (Ohtsuka *et*

al., 2008). The *pka1*Δ *sur2*Δ double mutant also showed a longer-lived phenotype than the *pka1*Δ mutant (Fig. 5A). However, because the *pka1*Δ *sur2*Δ double mutant grew more slowly than the *pka1*Δ and *sur2*Δ mutants, it was difficult to genetically assess the longevity phenotype. In addition, the *pka1*Δ *sur2*Δ double mutant was more sensitive to KCl and caffeine than the *pka1*Δ and *sur2*Δ mutants (Fig. S3). The *pka1*$^+$ and *sur2*$^+$ genes may function independently or in parallel on regulation of lifespan and responses to KCl and caffeine.

Next we analyzed the lifespan in response to caloric restriction (CR). As shown in Fig. 5B, wild type cells, *pka1*Δ mutant and *pka1*Δ *sur2*Δ mutant extended lifespan in response to CR, whereas *sur2*Δ mutant did not. The maximum lifespan extension under calorie restriction was observed in wild-type and *pka1*Δ mutant, but not in *sur2*Δ mutant. This indicated that *sur2*$^+$ is required for CR-dependent and *pka1*$^+$-independent lifespan extension. This again suggests that the *sur2*$^+$ and *pka1*$^+$ genes function independently or in parallel on lifespan regulation.

In *S. cerevisiae*, sphingolipids are known to be synthesized and modified by multiple enzymes (Fig. S1 and Nakase *et al*., 2010). In this study, we identified its orthologous gene, *sur2*$^+$, as one of the genes responsible for longevity in *S. pombe*. Because the composition of sphingolipids differs between *S. cerevisiae* and *S. pombe* (Fig. 3C), it is unclear whether the Sur2 protein catalyzes the same reaction in *S. pombe*. However, this finding indicates that the composition of sphingolipids may be one of the factors that determine yeast chronological lifespan. In this regard, it has been reported that treatment of *S. cerevisiae* with myriocin, which inhibits the synthesis of sphingolipid, extends chronological lifespan (Liu *et al*., 2013). However, no lifespan extension was observed when *S. pombe* was treated with myriocin (data not shown). Therefore, the mechanism of lifespan extension by myriocin and its universality are unknown. Sphingolipids are widely present in animal cells and are known to be involved in the construction of membrane microdomain (Van Meer and Simons 1988; Simons and Ikonen, 1997; Sturley, 2000; Gaigg *et al*., 2006). As mentioned above, we hypothesize that the imbalance caused by the decrease or increase of Sur2 activity may extend lifespan. Therefore, analysis of sphingolipid composition under both decreased and increased Sur2 states will contribute to the identification of sphingolipids involved in lifespan extension. Further analyses to elucidate the exact mechanism linking sphingolipids composition to lifespan are waiting in the future.

Acknowledgements

We are grateful to Dr. K. Takegawa (Kyusyu University) for helpful discussions. This study was supported by Japan Society for the Promotion of Science KAKENHI Grant Numbers 17H03792, 17K19227, 20H02898 (to HA). Part of this study was also supported by Institute for Fermentation, Osaka (to HA).

Conflict of interest

The authors declare that they have no conflicts of interest with the contents of this paper.

References

Bähler J, Wu JQ, Longtine MS, Shah NG, McKenzie A III, Steever AB, Wach A, Philippsen P, Pringle JR. (1998) Heterologous modules for efficient and versatile PCR-based gene targeting in *Schizosaccharomyces pombe*. *Yeast* **14:** 943-951.

Fabrizio P, Longo VD. (2003) The chronological life span of *Saccharomyces cerevisiae. Aging Cell* **2:** 73-81.

Fabrizio P, Pozza F, Pletcher SD, Gendron CM, Longo VD. (2001) Regulation of longevity and stress resistance by Sch9 in yeast. *Science* **292:** 288-290.

Fujita Y, Mita S, Ohtsuka H, Aiba H. (2007) Identification of a fatty acyl-CoA synthetase gene, *lcf2*$^{+}$, which affect viability after entry into the stationary phase in *Schizosaccharomyces pombe*. *Biosci. Biotech. Biochem*. **71:** 3041-3047.

Gaigg B, Toulmay A, Schneiter R. (2006). Very long-chain fatty acid-containing lipids rather than sphingolipids

per se are required for raft association and stable surface transport of newly synthesized plasma membrane ATPase in yeast. *J. Biol. Chem.* **281:** 34135-34145.

Imai Y, Shimasaki T, Enokimura C, Ohtsuka H, Tsubouchi, S, Ihara K, Aiba, H. (2020) *gas1* mutation extends chronological lifespan via Pmk1 and Sty1 MAPKs in *Schizosaccharomyces pombe. Biosci. Biotech. Biochem*. **84:** 330-337.

Ito H, Oshiro T, Fujita Y, Kubota S, Naito C, Ohtsuka H, Murakami H, Aiba H. (2010) Pma1, a P-type proton ATPase, is a determinant of chronological lifespan in fission yeast. *J. Biol. Chem.* **285:** 34616-34620.

Kondo N, Ohno Y, Yamagata M, Obara T, Seki N, Kitamura T, Naganuma T, Kihara A. (2014) Identification of the phytosphingosine metabolic pathway leading to odd-numbered fatty acids. *Nat. Commun*. **5:** 5338.

Kurauchi T, Hashizume A, Imai Y, Hayashi K, Tsubouchi S, Ihara K, Ohtsuka H, Aiba, H. (2017) Identification of a novel protein kinase that affects on the chronological lifespan in fission yeast. *FEMS Microbiology Letters* **364:** fnw257.

Liu J, Huang X, Withers BR, Blalock E, Liu K, Dickson RC. (2013) Reducing sphingolipid synthesis orchestrates global changes to extend yeast lifespan. *Aging Cell* **12:** 833-841.

Longo VD, Fabrizio P. (2002) Regulation of longevity and stress resistance: a molecular strategy conserved from yeast to humans? *Cell. Mol. Life Sci*. **59:** 903-908.

Longo VD, Kennedy BK. (2006) Sirtuins in aging and age-related disease. *Cell* **126:** 257-268.

Naito C, Ito H, Oshiro, Ohtsuka H, Murakami H, Aiba H. (2014) A new pma1 mutation identified in a chronologically long-lived fission yeast mutant. *FEBS Open Bio.* **4:** 829-833.

Nakase M, Tani M, Morita T, Kitamoto HK, Kashiwazaki J, Nakamura T, Hosomi A, Tanaka N, Takegawa K. (2010) Mannosylinositol phosphorylceramide is a major sphingolipid component and is required for proper localization of plasma-membrane proteins in *Schizosaccharomyces pombe*. *J. Cell Sci.* **123:** 1578-1587.

Ohtsuka H, Mita S, Ogawa Y, Azuma K, Ito H, Aiba H. (2008) A novel gene, *ecl1*$^{+}$, extends the chronological lifespan in fission yeast. *FEMS Yeast Res*. **8:** 520-530.

Ohtsuka H., Shimasaki T, Aiba H. (2020) Genes affecting the extension of chronological lifespan in *Schizosaccharomyces pombe* (fission yeast). *Mol. Microbiol.* DOI: 10.1111/mmi.14627

Oshiro T, Aiba H, Mizuno T. (2003) A defect in a fatty acyl-CoA synthetase gene, *lcf1*$^{+}$, results in a decrease in viability after entry into the stationary phase in fission yeast. *Mol. Genet. Genomics.* **269:** 437-442.

Roux AE, Chartrand P, Ferbeyre G, Rokeach LA. (2010) Fission yeast and other yeasts as emergent models to unravel cellular aging in eukaryotes. *J. Gerontol. A. Biol. Sci. Med. Sci.* **65:** 1-8.

Roux AE, Quissac A, Chartrand P, Ferbeyre G, Rokeach LA. (2006) Regulation of chronological aging in *Schizosaccharomyces pombe* by the protein kinases Pka1 and Sck2. *Aging Cell* **5:** 345-357.

Simons K, Ikonen E. (1997). Functional rafts in cell membranes. *Nature* **387:** 569-572.

Sturley SL. (2000). Conservation of eukaryotic sterol homeostasis: new insights from studies in budding yeast. *Biochem. Biophys. Acta* **1529:** 155-163.

Uemura S, Shishido F, Tani M, Mochizuki T, Abe F, Inokuchi J I. (2014). Loss of hydroxyl groups from the ceramide moiety can modify the lateral diffusion of membrane proteins in *S. cerevisiae*. *J. Lipid Res*. **55:** 1343–1356.

Van Meer G, Simons K. (1988). Lipid polarity and sorting in epithelial cells. *J. Cell Biochem*. **36:** 51-58.

Figure Legends

Fig. 1. The L1 mutant has a long-lived phenotype with increased cell viability after entering stationary phase. A. Cell growth (left panel) and cell viability (right panel) of wild type cells (open circles) and L1 mutant (open triangles) in SD medium. B. Sequencing data corresponding to the identified mutant loci of the *sur2*$^{+}$ gene. Representative data from the parental strain (HM3802), normal-lived F1 progeny, and long-lived F1 progeny after crosses are shown. The region corresponding to the *sur2-L1* mutation site is shaded. Note that the original GCT to GTT mutation resulted in a missense mutation from Ala-196 to Val in the Sur2 protein.

Fig. 2. The *sur2-L1* mutation in the L1 mutant causes a long-lived phenotype. A. The *sur2-L1* mutation in L1 mutant and the constructed *sur2-L1::kan*^{R} mutant are shown schematically. B. Cell growth (left panel) and cell viability (right panel) of wild type cells (open circles), L1 mutant (open triangles) and *sur2-L1::kan*^{R} mutant (open rectangles) in SD medium were monitored. Data shown are means ±s.d. of three independent experiments. C. Wild type (JY333) and L1 mutant cells were transformed with an empty vector (pLB-Dblet) or pSur2 plasmid carrying the *sur2*$^{+}$ gene. The cells were cultured in SD liquid medium for 1 day (Day1) and 3 days (Day3), then serially diluted and spotted on YE plate for viability analysis. The plates were incubated at 30 °C for 4 days and then photographed.

Fig. 3. TLC analysis of sphingolipids from yeast and various mutants. A. Domain composition of Sur2 protein and the region of *sur2-L1* mutation. B. GST-tagged Sur2 and Sur2-L1 proteins were expressed and monitored by Western blotting analysis. Tubulin was detected and used as a loading control. C. TLC analysis of sphingolipids from *sur2-L1::kan*^{R} mutants. *S. cerevisiae* (Sc) wild-type and *sur2*Δ, *S. pombe* (Sp) wild-type, *sur2-L1::kan*^{R} and *sur2*Δ cells were cultured and the lipids were extracted and analyzed. The positions of the various sphingolipid species are shown. The structure and abbreviation of each sphingolipid are shown in Fig. S1. * denotes unidentified bands.

Fig. 4. Other phenotypes of *sur2-L1::kan*^{R} and *sur2*Δ mutant. A. Cell growth (left panel) and cell viability (right panel) of wild type cells (open circles) and *sur2*Δ mutant (open rectangles) in SD medium were monitored. The data shown represent the mean ±s.d. of three independent experiments. B. Wild type cells, *sur2*Δ and *sur2-L1::kan*^{R} mutant were spotted in serial dilutions onto YE or YE plates containing 1M KCl or 10 mM caffeine. The plates were incubated at 30 °C for several days and then photographed. -, SS, and S show no difference, severe susceptibility and susceptible phenotypes, respectively, compared to wild-type cells.

Fig. 5. Analysis of genetic interaction between *sur2*$^{+}$ and *pka1*$^{+}$. A. Cell growth (left panel) and cell viability (right panel) of wild type cells (closed circles), *pka*1Δ (closed triangles), *sur2*Δ (closed rectangles) and *pka1*Δ *sur2*Δ mutants (crosses) in SD medium. B. Viability of the indicated mutant cells cultured in SD medium (closed circles) and SD low glucose medium (open circles). Data shown represent the mean ±s.d. of three independent experiments.

Supplemental Figure S1. Structure and biosynthetic pathway of sphingolipids in *S. cerevisiae*. The biosynthesis of sphingolipids begins with the condensation of palmitoyl-CoA and serine, which is synthesized in the endoplasmic reticulum to form ceramide (structure shown in middle). Ceramide is converted to IPC, MIPC and M(IP)2C. Due to the different hydroxylation states of ceramide (see table at the bottom), there are five species (ceramide types A, B, B', C and D) each of IPC. The sphingolipid long-chain base moiety of ceramides A and B' is dihydrosphingosine (DHS), while that of ceramides B, C and D is phytosphingosine (PHS). Sur2p is a sphingosine hydroxylase, capable of converting DHS to PHS and dihydroceramide to phytoceramide. Scs7p is a ceramide hydroxylase, capable of converting ceramide A to ceramide B' and ceramide B to ceramide C. The precise structure of sphingolipids and their enzymes in *S. pombe* have not yet known. Abbreviations are follows. IPC : inositol phosphorylceramide, MIPC : mannosylinositol phosphorylceramide, M(IP)2C : mannosyldiinositol phosphorylceramide. Genes responsible for the synthesis of sphingolipids in *S. cerevisiae* are shown. Orthologous genes in *S. pombe* are shown in parentheses. See Figure S2 for orthologous relationships between *S. pombe* and *S. cerevisiae*.

Supplemental Figure S2. Orthologous relationship between *S. pombe* and *S. cerevisiae*. *imt1*$^{+}$, *imt2*$^{+}$ and *imt3*$^{+}$ of *S. pombe* are the orthologues of *CSH1* and *SUR1* of *S. cerevisiae*. See Figure S1 for possible biosynthetic pathways.

Supplemental Figure S3. Similar phenotypes of *pka1*Δ and *sur2*Δ mutants. Wild type cells, *pka*1Δ, *sur2*Δ and *pka1*Δ *sur2*Δ mutant were spotted in serial dilutions onto YE plate or YE plate containing 1M KCl or 10 mM caffeine. The plates were incubated at 30 °C for 3 days and photographed.

A

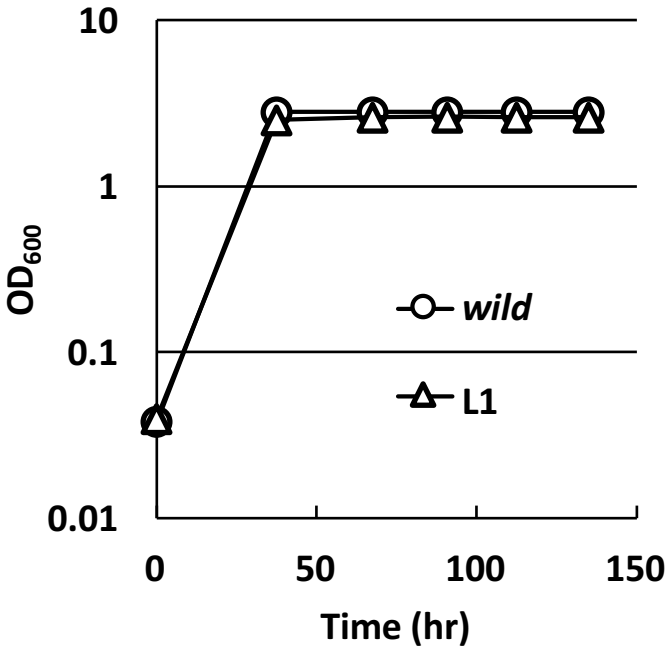

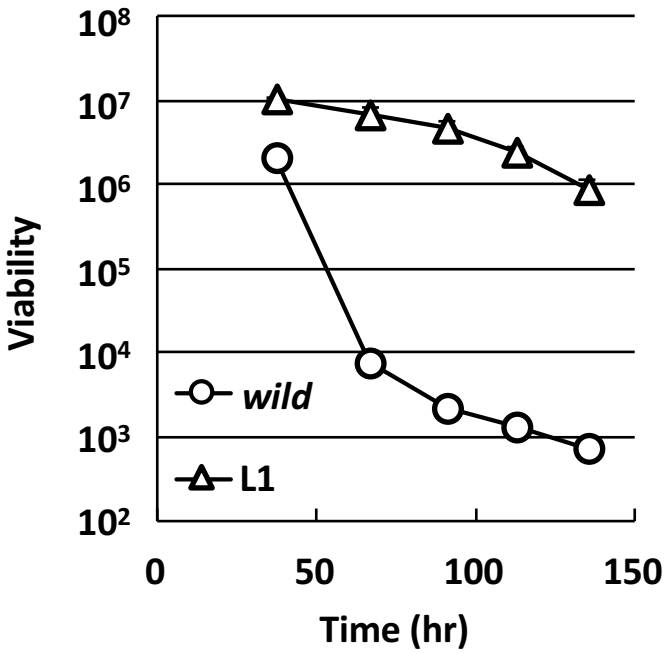

B

Parent strain (HM3802)

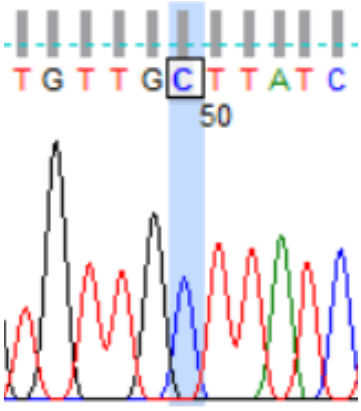

Normal lived F1

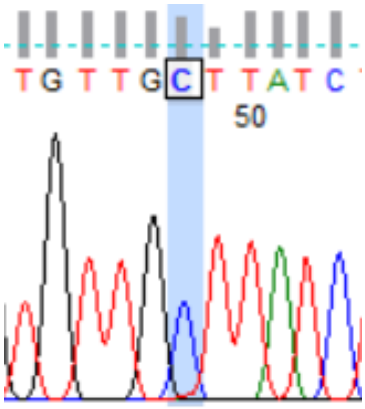

Long lived F1

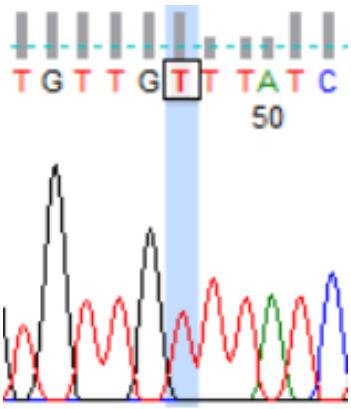

Fig. 1

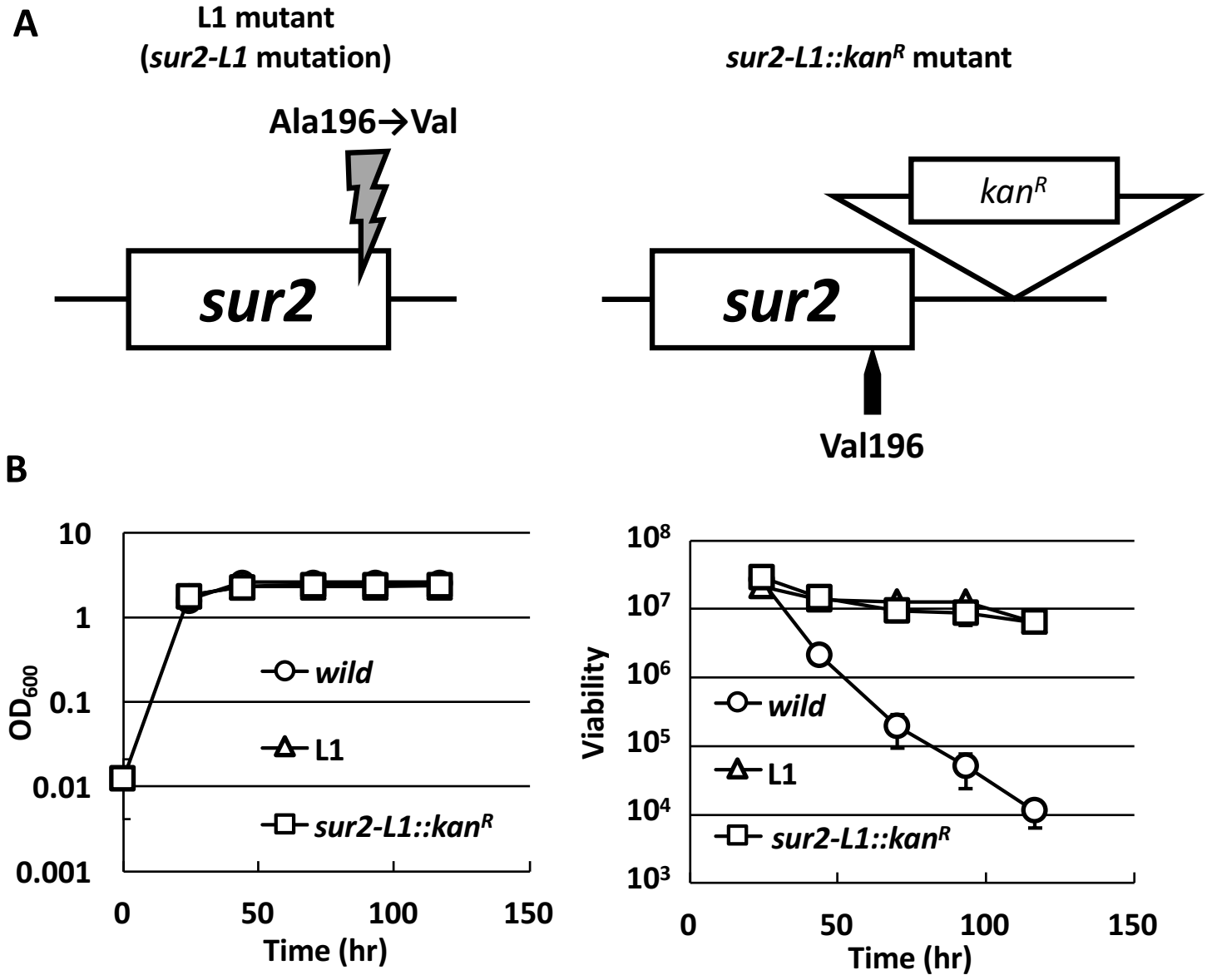
A
L1 mutant
(sur2-L1 mutation)
sur2-L1::kanR mutant
Ala196→Val
sur2
kanR
sur2
Val196
B
OD600
10
1
0.1
0.01
0.001
wild
L1
sur2-L1::kanR
0
50
100
150
Time (hr)
Viability
10^8
10^7
10^6
10^5
10^4
10^3
wild
L1
sur2-L1::kanR
0
50
100
150
Time (hr)

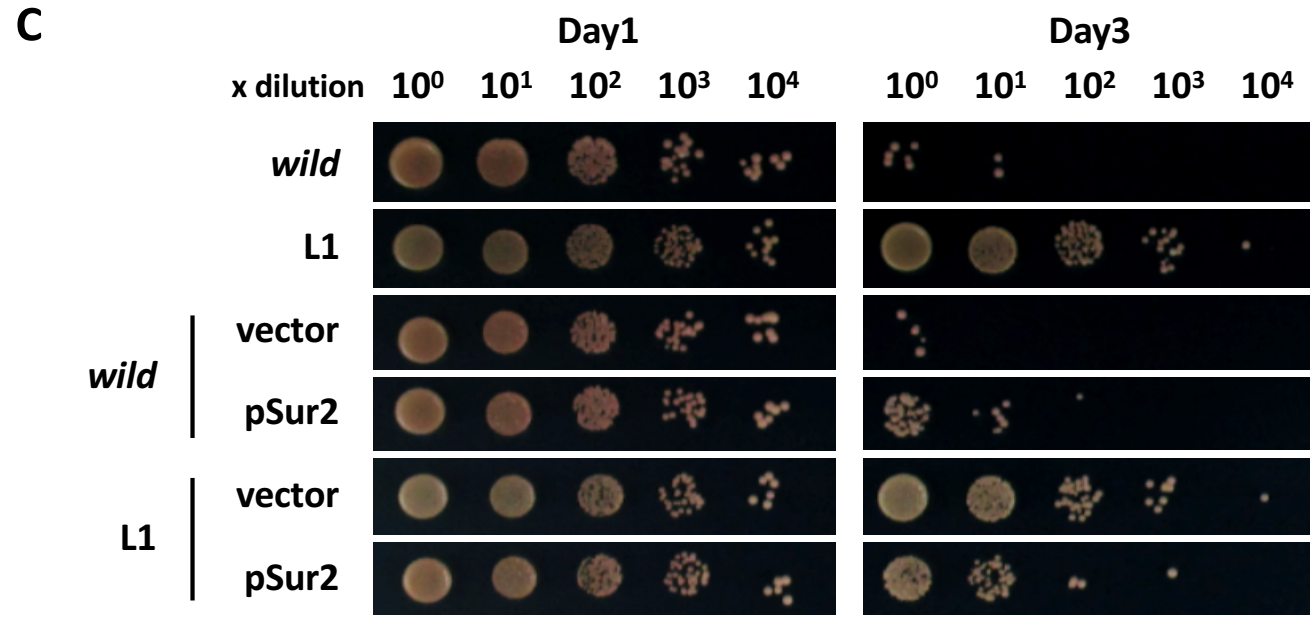
C
Day1
Day3
x dilution
10^0
10^1
10^2
10^3
10^4
wild
L1
wild
vector
pSur2
L1
vector
pSur2

Fig. 2

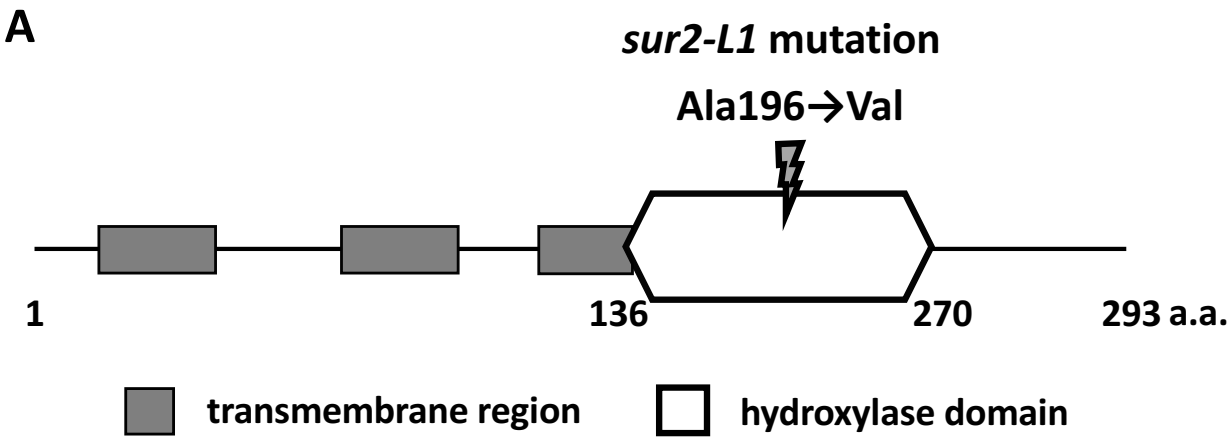
A
sur2-L1 mutation
Ala196→Val
1
136
270
293 a.a.
transmembrane region
hydroxylase domain

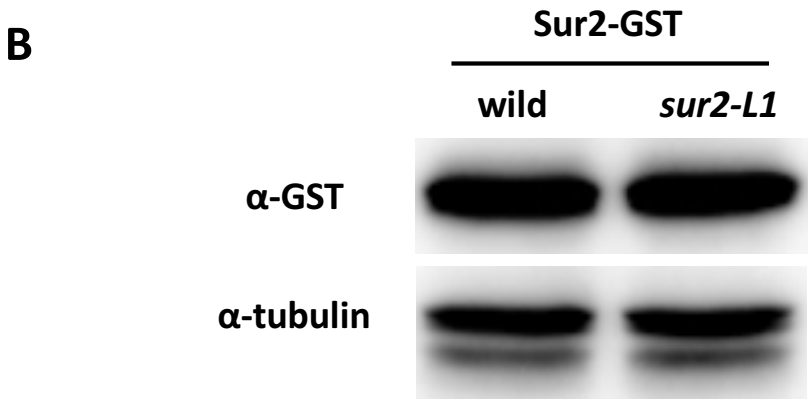
B
Sur2-GST
wild
sur2-L1
α-GST
α-tubulin

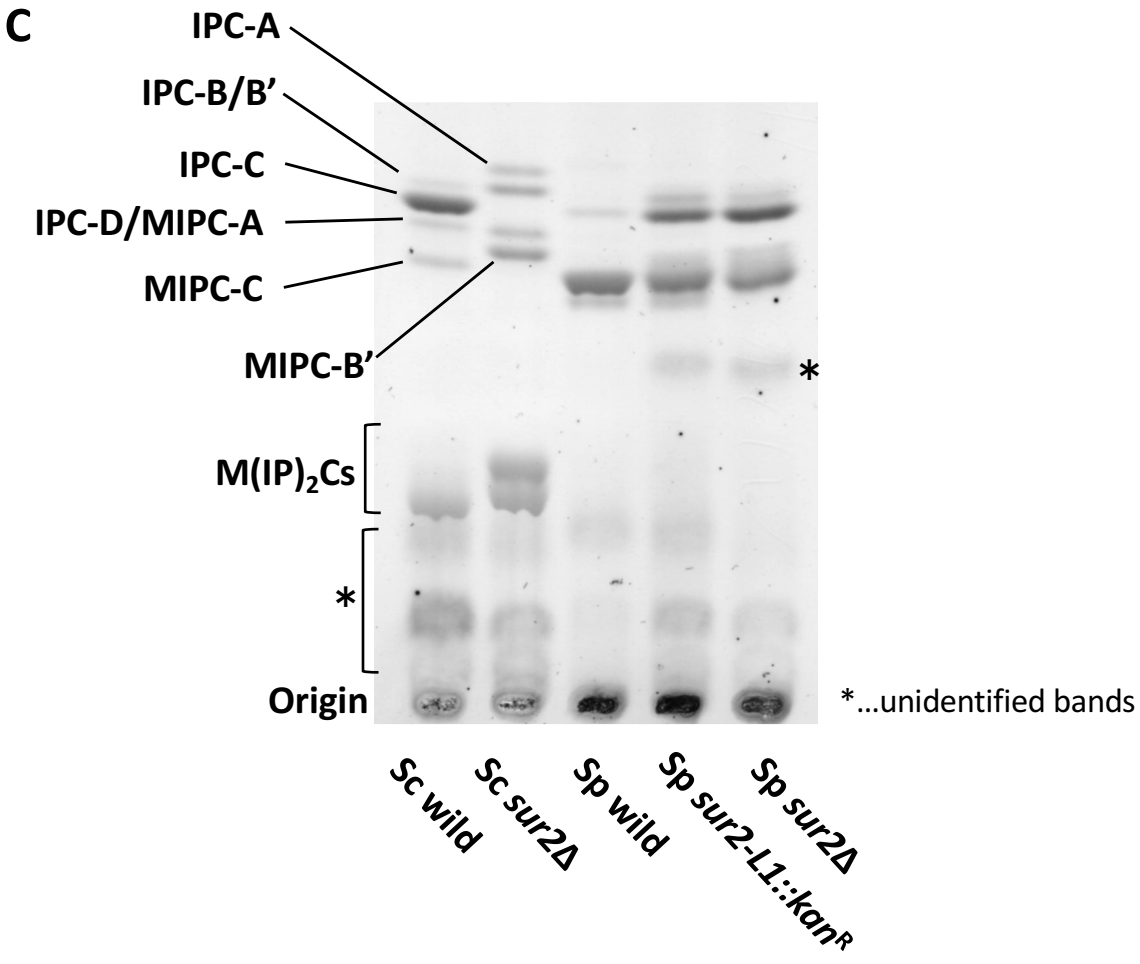
C
IPC-A
IPC-B/B'
IPC-C
IPC-D/MIPC-A
MIPC-C
MIPC-B'
M(IP)2Cs
*
Origin
*…unidentified bands
Sc wild
Sc sur2Δ
Sp wild
Sp sur2-L1::kanR
Sp sur2Δ

Fig. 3

A

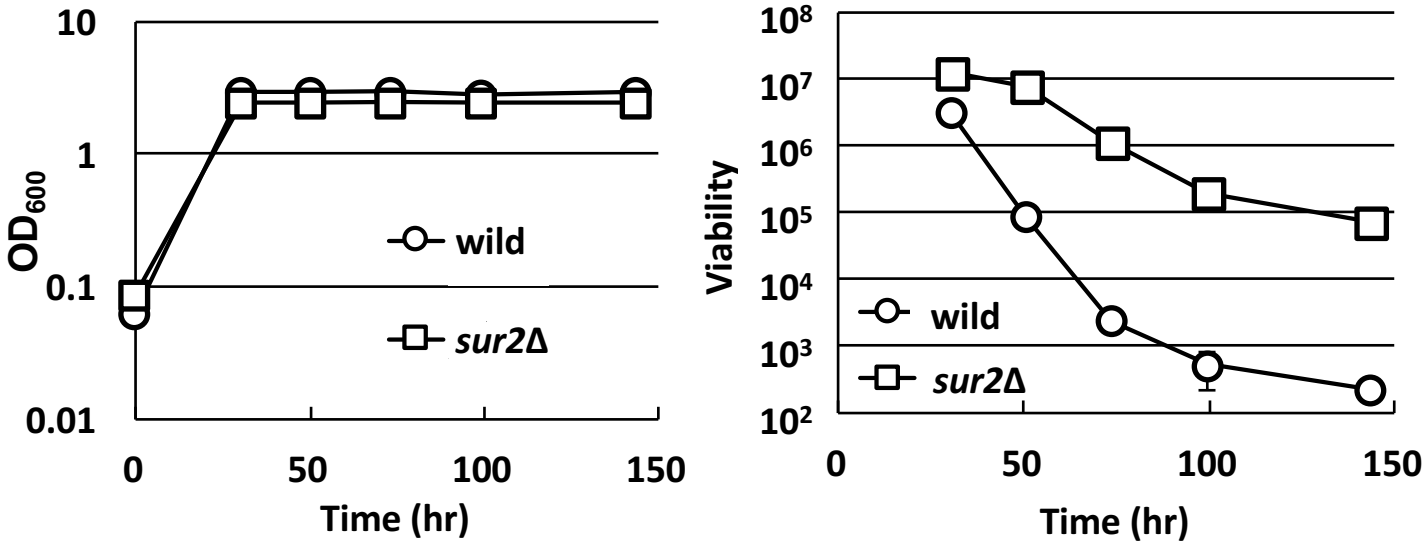
10
1
0.1
0.01
OD600
wild
sur2Δ
0
50
100
150
Time (hr)
10^8
10^7
10^6
10^5
10^4
10^3
10^2
Viability
wild
sur2Δ
0
50
100
150
Time (hr)

B

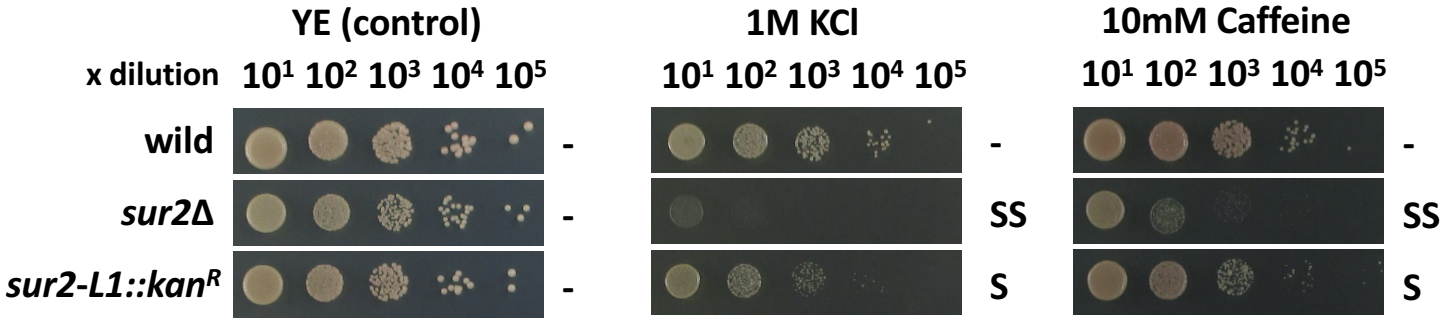
YE (control)
1M KCl
10mM Caffeine
x dilution
10^1 10^2 10^3 10^4 10^5
10^1 10^2 10^3 10^4 10^5
10^1 10^2 10^3 10^4 10^5
wild
sur2Δ
sur2-L1::kan^R
-
-
SS
S
-
SS
S

Fig. 4

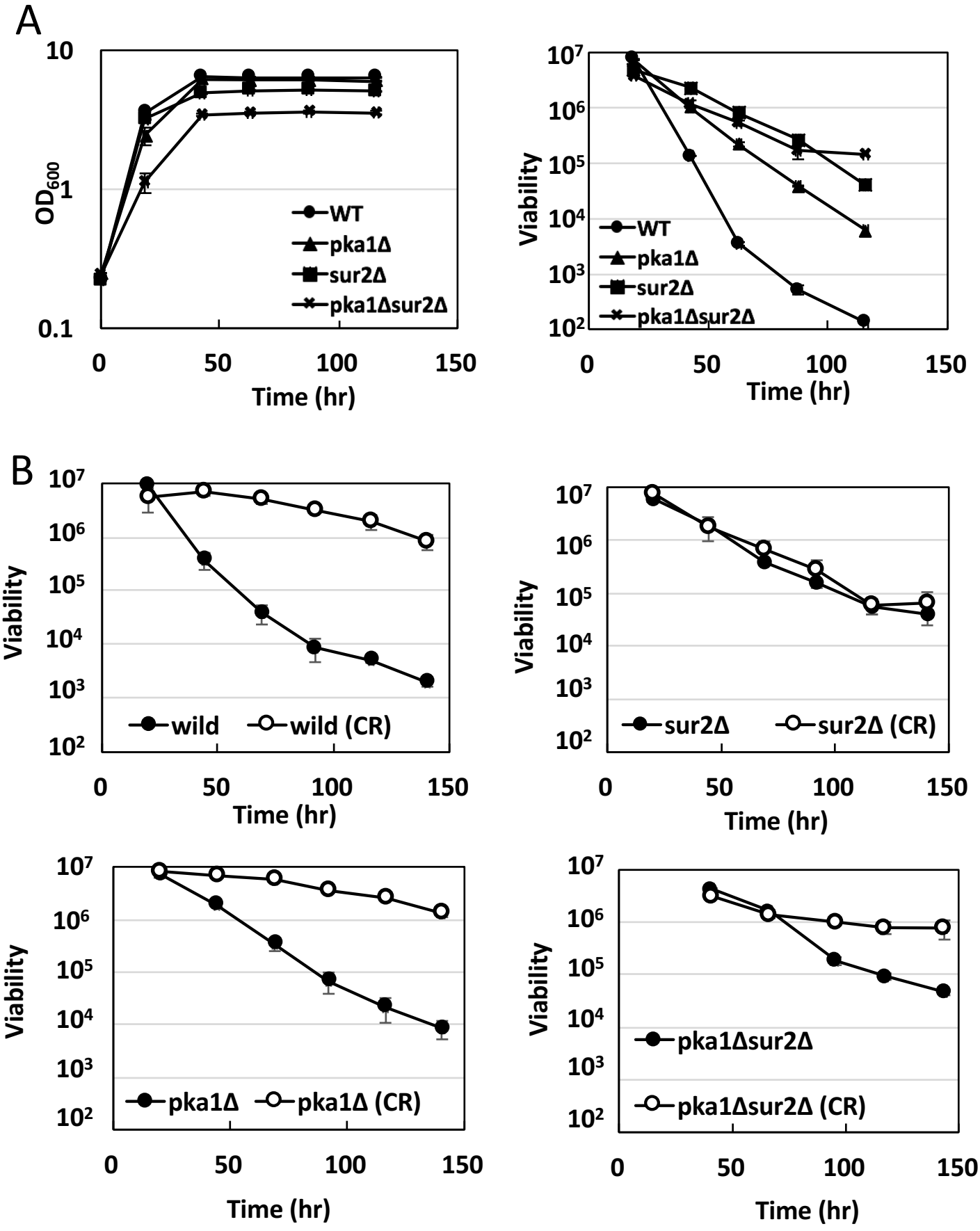
A
10
1
0.1
OD600
WT
pka1Δ
sur2Δ
pka1Δsur2Δ
0
50
100
150
Time (hr)
10^7
10^6
10^5
10^4
10^3
10^2
Viability
WT
pka1Δ
sur2Δ
pka1Δsur2Δ
0
50
100
150
Time (hr)
B
Viability
wild
wild (CR)
0
50
100
150
Time (hr)
Viability
sur2Δ
sur2Δ (CR)
0
50
100
150
Time (hr)
Viability
pka1Δ
pka1Δ (CR)
0
50
100
150
Time (hr)
Viability
pka1Δsur2Δ
pka1Δsur2Δ (CR)
0
50
100
150
Time (hr)

Fig. 5

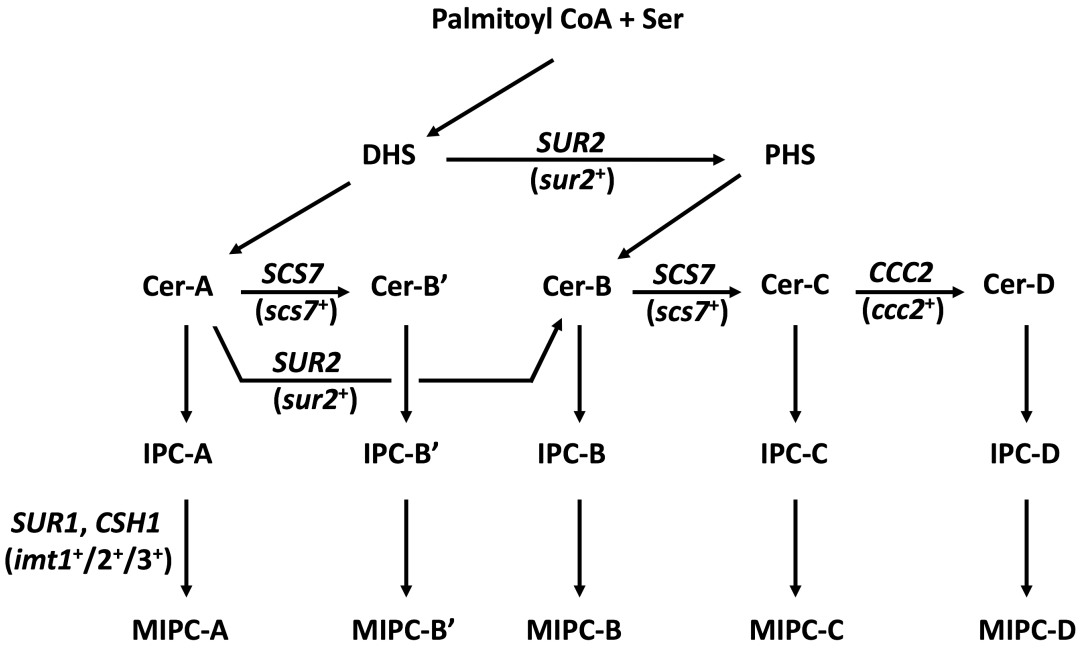

R=	Inositol-P-	IPC
	Mannose-inositol-P-	MIPC
	Inositol-P-mannose-inositol-P-	$M(IP)_2C$
	(P : phosphate)	

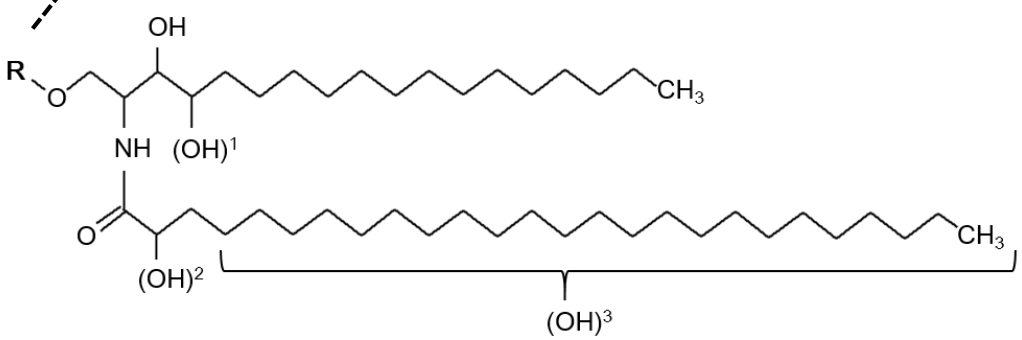

Location of the hydroxylation	A-type	B-type	B'-type	C-type	D-type
$(OH)^1$	-	-	+	+	+
$(OH)^2$	-	+	-	+	+
$(OH)^3$	-	-	-	-	+

Fig. S1

S. pombe			***S. cerevisiae***		
Gene Name	Systematic ID	Function	Gene Name	Systematic ID	Function
sur2+	SPBC887.15c	Sphingosine hydroxylase	*SUR2*	YDR297W	Sphinganine C4-hydroxylase
scs7+	SPAC19G12.08	ER sphingosine hydroxylase	*SCS7*	YMR272C	Sphingolipid alpha-hydroxylase
ccc2+	SPBC29A3.01	Golgi copper transporting ATPase (predicted)	*CCC2*	YDR270W	Cu(+2)-transporting P-type ATPase
imt1+	SPAC2F3.01	Mannosyl-transferase	*CSH1*	YBR161W	Mannosylinositol phosphorylceramide synthase
imt2+	SPCC4F11.04c		*SUR1*	YPL057C	
imt3+	SPAC17G8.11c				

Fig. S2

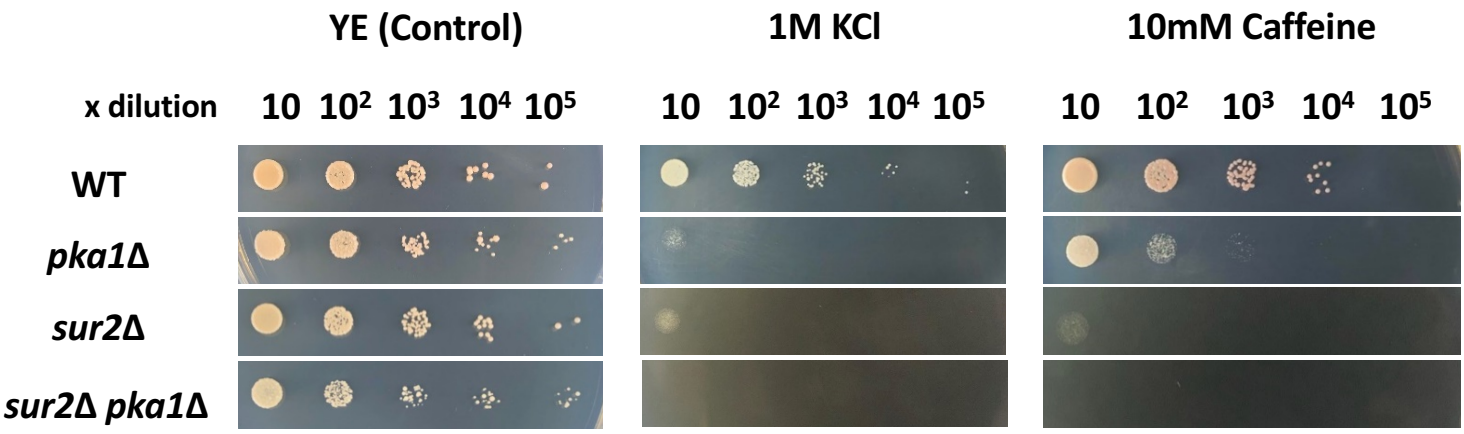
YE (Control)
1M KCl
10mM Caffeine
x dilution
10 10² 10³ 10⁴ 10⁵
10 10² 10³ 10⁴ 10⁵
10 10² 10³ 10⁴ 10⁵
WT
pka1Δ
sur2Δ
sur2Δ pka1Δ

Fig. S3